# Investigation of $AlMe_3$, $BEt_3$ and $ZnEt_2$ as Co-Reagents for Low-Temperature Copper Metal ALD / Pulsed-CVD

*Balamurugan Vidjayacoumar,*[†] *David J. H. Emslie,*[†]* *Scott B. Clendenning,*[‡]* *James M. Blackwell,*[‡]
*James F. Britten*[†] *and Arnold Rheingold*[§]

[†] Department of Chemistry, McMaster University, 1280 Main Street West, Hamilton, ON, L8S 4M1, Canada. Fax: (905)-522-2509; Tel: (905)-525-9140 x 23307. E-mail: emslied@mcmaster.ca

[‡] Intel Corporation, RA3-252, 2511 NW 229th Ave., Hillsboro, OR 97124, USA.

[§] Department of Chemistry and Biochemistry, University of California - San Diego, 9500 Gilman Drive, MC 0332, La Jolla, CA, 92093-0332.

**RECEIVED DATE**

**Abstract:** The reactions of $AlMe_3$, $BEt_3$ and $ZnEt_2$ with toluene solutions of the copper(II) complexes [$CuL_2$] {L = acetylacetonate (acac; **1**), hexafluoroacetylacetonate (hfac; **2**), *N*-isopropyl-β-ketiminate (acnac; **3**), *N*,*N*-dimethyl-β-diketiminate (nacnac; **4**), 2-pyrrolylaldehyde (PyrAld; **5**), *N*-isopropyl-2-pyrrolylaldiminate ($PyrIm^{iPr}$; **6a**), *N*-ethyl-2-pyrrolylaldiminate ($PyrIm^{Et}$; **6b**) and *N*-isopropyl-2-salicylaldiminate (IPSA; **7**)} were investigated, and most combinations were found to deposit metal films or metal powder at 50 °C or less. SEM and XPS of metal films deposited on ruthenium showed a range of morphologies and compositions, including pure copper (excluding oxygen content after atmospheric exposure). These non-aqueous solution screening studies provided a rapid and convenient means to identify the most promising [$Cu^{II}L_2$] precursor / $ER_n$ co-reagent combinations for copper metal ALD/pulsed-CVD studies, and subsequent ALD/pulsed-CVD studies were performed using **6b** in combination with $AlMe_3$, $BEt_3$ and $ZnEt_2$. As in solution, the reactivity of these reagents (pulsed-CVD) followed the order $ZnEt_2 \sim AlMe_3 >> BEt_3$. Furthermore, at 120 to 150 °C, $ZnEt_2$ was used successfully to deposit smooth, conductive films composed of copper with 8–15% Zn. Based on CVD studies with $ZnEt_2$, zinc content appears to derive from a parasitic CVD process, which becomes more favorable above 120 °C, detracting from the goal of self-limiting deposition.

**Introduction:** Ultra-thin metal films have a wide variety of applications in integrated circuits, magnetic information storage, fuel cells and catalysis. Copper, which is the focus of this work, has now replaced aluminum as the primary interconnect metal for most microelectronics applications, largely due to improvements in reliability, speed and scaleability which result from lower resistivity and increased resistance to electromigration.[1,2] Since interconnect metals must be deposited into high aspect ratio holes and trenches with ever decreasing top dimensions, highly conformal copper deposition is required in order to ensure complete filling of these features. Processes which have been used to deposit ultra-thin copper films or copper seed layers include physical vapor deposition (PVD), chemical vapor deposition (CVD), electrodeposition (typically onto a pre-existing conformal copper seed layer) and electroless deposition.[1,3] However, all of these approaches face increasing challenges in terms of conformality and uniformity as critical dimensions decrease and aspect ratios increase,[4] so new processes to allow more uniform and conformal copper metal deposition will likely be required.[5]

The process of atomic layer deposition (ALD), also referred to as atomic layer epitaxy (ALE), is a particularly promising method for the deposition of highly-conformal, uniform thickness, ultra-thin films of the type required in future microelectronics devices. ALD is related to the process of CVD, in that the metal source is a volatile metal complex. However, deposition is achieved not by thermal decomposition of a metal complex on a heated substrate surface (CVD), but by repeated alternating surface controlled reactions between a metal precursor and a co-reactant, at least one of which is adsorbed on the substrate surface during the nucleation process to initiate ALD film growth.

In a typical ALD process, the metal precursor is chemisorbed on the film surface in a self-limiting fashion (at a temperature at which CVD does not occur), and any excess precursor and volatile byproducts are removed with an inert gas purge. Vapors of a volatile co-reagent (e.g. $H_2$, $O_2$, $H_2O$, $H_2S$ or $NH_3$) are then introduced to the surface, and react with the chemisorbed metal precursor to deposit the desired material (e.g. a metal or metal oxide film), effect the release of volatile byproducts, and create a suitable surface functionalization to allow reaction in the next metal precursor vapor exposure.

The surface reaction with the co-reagent is also self-limiting and excess co-reagent and volatile byproducts are removed with an inert gas purge. In this fashion, so long as sufficient vapor doses of the metal precursor and co-reagent are delivered to ensure maximum surface coverage and complete reaction, the film thickness will depend only on the number of precursor/purge/co-reagent/purge cycles, and the film will grow conformally on all exposed surfaces on which nucleation can occur. If self-limiting behaviour cannot be achieved (even in cases where ALD reactivity is accompanied by a minor parasitic CVD process), the overall process is termed pulsed-CVD, although the experimental setup is identical to that for ALD.[5-7]

The material deposited in ALD is typically elemental metal with $H_2$ or $O_2$ (only in the case of noble metals such as Rh, Ir, Pd & Pt),[5] a metal oxide with $H_2O$ or $O_3$,[7,8] a metal nitride with $NH_3$ or $RNH_2$,[5] a metal sulphide with $H_2S$,[9] and a metal selenide or telluride with $H_2Se$, $Se(SiR_3)_2$ or $Te(SiR_3)_2$.[10,11] However, while ALD of a wide range of metal oxides and nitrides has been demonstrated, ALD of metals is far less common (Table S1 in supporting information).[12-22] One reason for this is the very limited selection of co-reagents currently available for ALD of metal films. In addition, the strongly reducing or oxidising nature of these reagents (especially at high temperatures) significantly limits the range of substrates compatible with metal ALD. Further, the requirement for high temperatures (typically 200-400 °C) precludes the use of metal ALD on many less-thermally robust substrates, has the potential to cause de-wetting leading to discontinuous films,[23,24] and greatly reduces the number of suitable metal precursors, since thermal decomposition leading to CVD rather than ALD must be avoided.

For thermal copper metal ALD, initial reports involved $H_2$ in combination with CuCl at 360-410 °C,[21] $[Cu(thd)_2]$ (thd = 2,2,6,6-tetramethyl-3,5-heptanedionate) at 190-260 °C,[20] and $[Cu(acac)_2]$ at 250 °C.[19] More recently, Gordon *et al.* reported the use of a liquid copper amidinate precursor, $[Cu_2\{({}^{s}BuN)_2CMe\}_2]$ which allowed ALD with $H_2$ at temperatures in the range 150–190 °C;[13] much lower than achieved with $[Cu_2\{({}^{i}PrN)_2CMe\}_2]$ (280 °C).[17,18] Plasma-enhanced ALD (PEALD)[25] has

also been investigated for metal deposition, but this technique requires more complex ALD reactors, is often considered less suitable for deposition on substrates with high aspect-ratio features due to rapid recombination of radical species, and can lead to substrate surface damage.[5,17] In addition, indirect approaches to metal ALD have been reported, including ALD of $Cu_3N$ followed by conversion to copper metal by treatment with $H_2$ at 160 °C,[26] and ALD of CuO followed by conversion to copper metal, either electrochemically in an aqueous solution of a metal hydroxide, or by treatment with reagents such as $H_2$ (270-320 °C), H-plasma (150-300 °C), CO, ROH, formalin, RCHO or $RCO_2H$.[27]

Deposition of copper metal at temperatures well below 200 °C has been reported using copper(I)[14,28] or copper(II)[15,29] β-diketiminate precursors in combination with $H_2SiEt_2$, both in solution and by exposure of films of the copper complexes to diethylsilane.[30] However, the effectiveness of this co-reagent (and the temperatures that would be required) to effect copper metal deposition from the copper(II) precursors under realistic ALD conditions was not disclosed, and a recent report has demonstrated a pulsed-CVD mechanism, rather than an ALD mechanism, for copper deposition using [(nacnac)Cu($H_2C$=$CHSiMe_3$)] {nacnac = $(CH_2)_3$N-C=CH-CMe=NH} with $H_2SiEt_2$.[31] Proof-of-concept studies on copper film deposition using copper(II) pyrrolylaldiminate complexes with $H_2SiEt_2$ (160-170 °C) or a 1:1 mixture of $H_2$ and $NH_3$ (≥180 °C) have also been described.[16] Additionally, copper metal (containing 5-16 % carbon) deposition at temperatures between 25 and 100 °C was recently reported using sequential pulses of [Cu(hfac)$_2$], pyridine and $H_2$. Pyridine is proposed to interact with surface-bound Cu(hfac)$_2$ to weaken the Cu–O bonds and facilitate reduction by $H_2$. However, self-limiting film growth was not reported.[32] The most prominent example of low temperature copper metal ALD was published during the course of this work by Sung and Fischer *et al.*, and involves reaction of bis(*N*,*N*-dimethyl-2-aminoisopropoxide)copper(II) with $ZnEt_2$ at 100 - 120 °C. Copper films were deposited: (a) on oxidized Si(100) substrates with a growth rate of 0.2 Å/cycle, (b) on an oxidized silicon substrate patterned with alkyl siloxane SAMs, and (c) inside the pores of a nanoporous polycarbonate membrane,

providing copper nanotubes after treatment with chloroform.[12] This work marks the emergence of a new class of co-reagent for late transition metal ALD.

Herein we report the use of solution deposition studies as a means to identify particularly promising metal precursor / co-reagent combinations for metal ALD or pulsed-CVD. These studies are rapid and straightforward, unlike ALD/pulsed-CVD studies, which are time consuming, resource intensive, and require the use of highly specialized equipment. Co-reagents investigated in this work are $AlMe_3$, $BEt_3$ and $ZnEt_2$, and studies into the potential of these co-reagents for copper metal ALD/pulsed-CVD are described.

## Results and Discussion

**Co-Reagent Selection:** The homoleptic alkyl compounds $AlMe_3$, $BEt_3$ and $ZnEt_2$ were investigated as co-reagents to allow copper metal ALD/pulsed-CVD under mild conditions {low temperatures (100-200 $^{o}$C) and the absence of strong, unselective reducing or oxidising agents}. Their Lewis acidity, compatability with hard N- and O-donor ligands, and alkylating ability makes them excellent candidates to convert $CuL_2$ precursors to 'LCuR', '$CuR_2$' and/or 'CuR' (R = Me, Et or H) complexes, which can be expected to undergo facile decomposition leading to copper metal; detailed investigations into the pathway responsible for solution-deposition of copper metal are described in the subsequent companion article.[33] The co-reagents $AlMe_3$, $BEt_3$ and $ZnEt_2$ are also inexpensive, thermally stable, volatile, and liquid at room temperature,[34] so are readily deliverable in an ALD or pulsed-CVD process. Furthermore, they are expected to be more selective in the initiation of reduction processes than $H_2$ or compounds containing E-H (E = B, Al, Si etc.) bonds, and the use of liquid, rather than gaseous co-reagents allows solution screening studies to be performed in an efficient semi-combinatorial fashion (inside an inert-atmosphere workstation), prior to ALD/pulsed-CVD studies.

**Copper Precursor Complexes:** All copper precursors investigated in this work are of the form [$Cu^{II}L_2$], where L is acetylacetonate (acac; **1**),[35] hexafluoroacetylacetonate (hfac; **2**),[36,37] *N*-isopropyl-β-ketiminate (acnac; **3**), *N*,*N*-dimethyl-β-diketiminate (nacnac; **4**),[15,38] 2-pyrrolylaldehyde (PyrAld; **5**),[39] *N*-isopropyl-2-pyrrolylaldiminate ($PyrIm^{iPr}$; **6a**), *N*-ethyl-2-pyrrolylaldiminate ($PyrIm^{Et}$; **6b**)[16,40] and *N*-isopropyl-2-salicylaldiminate (IPSA; **7**)[41,42] (Figure 1). Complexes **1**[35] and **2**[37,43] are square planar, while **7**[42] deviates towards tetrahedral geometry with an inter-ligand angle of 59 degrees. The solid state structures of **4, 6a** and **6b** have not been reported. However, based on related structures in the literature (ESI Table 1), and bearing in mind that more effective electron donation and increased steric hindrance have been reported to result in greater distortion towards tetrahedral geometry in

$[CuL_2]$ (L = 2-pyrrolylaldimine) complexes,[16] inter-ligand tilt angles of ~60° for **4**,[15] 45-55° for **6a** and 40-45° for **6b**[16,44] can be expected.

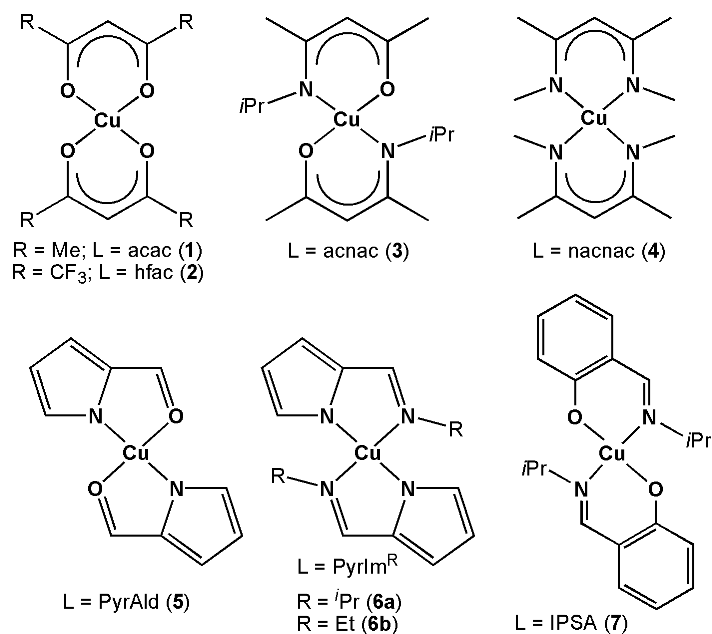


**Figure 1.** Homoleptic copper(II) complexes **1-7**.

X-ray quality crystals of **3** were obtained from hexanes at –30 °C, and confirmed that the complex is 4-coordinate,[45] with an inter-ligand tilt angle of 59 degrees (Figure 2). The Cu-O bond distance of 1.916(1) Å is similar to those observed in $[Cu(acac)_2]$ (**1**) [1.912(4) and 1.914(4) Å],[35] and the Cu-N bond distance of 1.974(2) Å is only slightly longer than those observed in $[CuL_2]$ (L = *N*-methyl-*N*'-ethyl-β-diketiminate; Cu-N 1.93–1.95 Å).[15] X-ray quality crystals of **5** were prepared by slow evaporation of a diethyl ether solution at room temperature. Complex **5** is square planar, as are **1** and **2** which are similarly free from unfavorable inter-ligand steric interactions (Figure 3). The anionic N-donors in **5** are *trans*-disposed, and the Cu-N bond distance [1.918(2) Å] is slightly shorter than those typically observed for pyrrolylaldimine complexes (1.93-1.96 Å).[16]

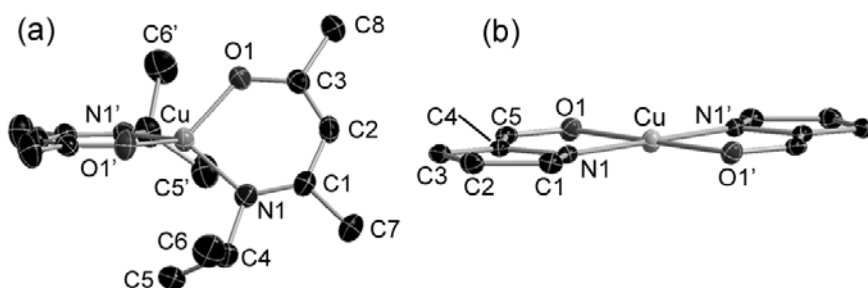


**Figure 2.** Solid state structure of complexes **3** (a) and **5** (b) with thermal ellipsoids at 50 %. Hydrogen atoms are omitted for clarity.

Complexes **1**-**7** were selected due to ease of synthesis, reasonable thermal stability and volatility (in most cases), and for **1**, **2** and **4**, reported use in copper metal CVD and/or ALD. They also represent a variety of different ligand types, differing in donor-set, the extent of electron delocalization, and steric/electronic properties. Thermogravimetric analyses (TGA) for the less well-studied complexes in the group (**3**-**7**) are shown in Figure 3; it is believed that weight loss is primarily due to decomposition with volatilization of the organic byproducts and not vaporization of the copper complex itself, with the possible exception of complex **7**. The most thermally robust precursor is **7** and the least robust is **4**, with all other complexes showing an onset of decomposition at 170-220 °C. Under a vacuum of 1 x $10^{-3}$ torr, sublimation temperatures for the complexes studied were: 120 °C for **1**, <20 °C for **2**, 80 °C for **3**, 80 °C (with accompanying decomposition) for **4**, 120 °C for **6a**, 90 °C for **6b** and 120 °C for **7** (complex **5** was not volatile).

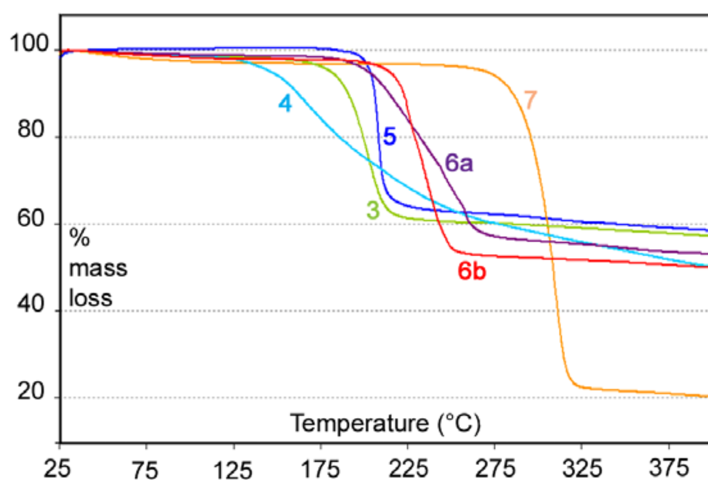


**Figure 3.** Thermogravimetric analyses (TGA) for complexes **3-7** under an argon atmosphere. The temperature was increased at a rate of 10 °C per minute.

**Solution screening studies:** Our approach to the development of new low temperature methods for copper metal ALD/pused-CVD focused on the initial application of non-aqueous solution screening experiments. These experiments could be conducted rapidly and in parallel, with visual identification of metal film and metal powder deposition and subsequent analysis by SEM, XPS and/or PXRD to confirm that deposited material was largely composed of copper. This approach provided an efficient and straightforward means to probe the extent to which the primary steps for copper metal deposition occur in the temperature range most relevant to new low-temperature ALD/pulsed-CVD method development (25–120 °C), and to determine the most promising copper precursor / co-reagent combinations for subsequent ALD/pulsed-CVD studies. Solution reactions also provide a valuable opportunity for detailed mechanistic studies using a range of powerful and readily accessible characterization techniques,[46] and the pathways responsible for copper metal deposition in the solution reactions of **6a** with $AlMe_3$, $BEt_3$ and $ZnEt_2$ are discussed in a subsequent companion article.[33]

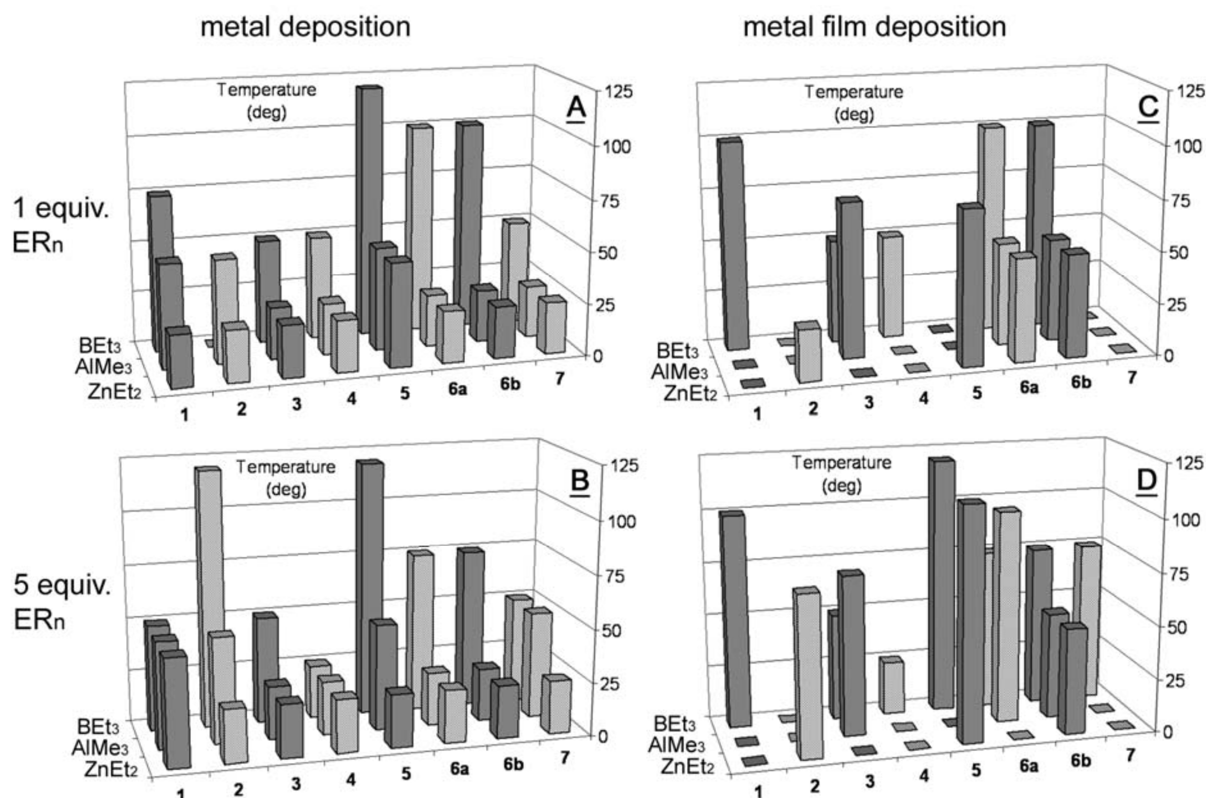


**Figure 4.** Minimum temperatures for: (A and B) deposition of a copper-containing film and/or powder, and (C and D) deposition of a copper-containing film.[47] Graphs A and C correspond to 1:1 reactions of complexes **1**-**7** with $AlMe_3$, $BEt_3$ and $ZnEt_2$, while graphs B and D correspond to reactions with 1:5 stoichiometry. Solutions were 13.6 mM (1.1 mL total volume; A and C) or 10 mM (1.5 mL total volume; B and D) in copper complex, and reactions were maintained for 24 hours at each of the following temperatures in sequence: 25, 50, 75, 100, 120 °C. The x-axis refers to metal complex (**1**-**7**), the y-axis (vertical) refers to deposition temperature, and the z-axis indicates the co-reagent employed ($BEt_3$, $AlMe_3$ or $ZnEt_2$). Bars at the baseline on the graphs correspond to complexes which did not deposit metal (graphs A and B) or a metal film (graphs C and D) within the temperature range studied.

Solution screening studies were performed by maintaining toluene solutions of **1**-**7** with $AlMe_3$, $BEt_3$ or $ZnEt_2$ (1 and 5 equiv) for 24 hours at each of the following temperatures in sequence: 25, 50,

75, 100 and 120 °C. Deposition of either a copper-colored metal film or precipitation of a black or copper-colored powder was observed at 25-50 °C in >85 % of the reactions (Figure 4), and in some cases, solution color changes were observed at 25 °C, prior to metal deposition. The latter observation indicates disappearance of [$CuL_2$] prior to, rather than concurrent with metal deposition. For example, addition of $AlMe_3$ and $ZnEt_2$ to **6a** led to immediate consumption of the copper(II) precursor, even at –78 °C, although significant copper metal deposition was not observed until the temperature was raised to –20 °C for $ZnEt_2$ and 20 °C for $AlMe_3$.[48] In contrast to the high observed reactivity of the organoaluminum and zinc reagents, $BEt_3$ reacted only slowly with **1**-**7**, even at 50 to 75 °C.

Metal powders deposited in the reactions of **1-7** with $AlMe_3$, $BEt_3$ and $ZnEt_2$ were shown to be composed of copper (within the limits of detection by PXRD, which does not include amorphous materials), with the exception of that from **7** with $ZnEt_2$, which was identified as mixture of amorphous Zn (84%) and brass (β-CuZn;16%)[49] by a combination of PXRD and XPS.[50] Metal precursor / $ER_n$ co-reagent reactions resulting in the formation of a metal *film* (7 combinations using $BEt_3$, 3 with $AlMe_3$ and 4 with $ZnEt_2$) were repeated in the presence of $Si/SiO_2/Ta/Ru$ wafer sections, and the resulting films were analyzed by XPS after initial sputtering to remove higher levels of oxidized material and organic impurities at the surface.

SEM images for a selection of the films are provided in Figure 5, and elemental composition (by XPS) is provided in the supplementary information. These data are of independent interest from the perspective of metal film solution deposition, and an understanding of film morphology is also valuable for the interpretation of XPS data. However, the morphology of solution-deposited films is not expected to correlate with film morphologies observed by ALD or pulsed-CVD. Key findings were: (1) All but one film showed good adhesion to the substrate, as determined by a standard tape test. (2) Films were 10-300 nm thick and of varied morphology; from dense solid films with an undulating surface, to continuous films of densely-packed approximately spherical 5-35 nm grains, to a loosely-packed layer of 30-130 nm diameter platelet-shaped granules (Figure 5). (3) Copper films deposited using $BEt_3$

contained very low levels of boron (0-1.5 at%) and did not contain nitrogen at levels detectable by XPS (~ 0.5 at%). (4) Metal films deposited using $AlMe_3$ contained < 0.5 at% N, but significant amounts of Al; from 8% to 42% Al in Cu. (5) Films deposited using $ZnEt_2$ contained varying amounts of Zn, with compositions ranging from 2.5% Zn in Cu, to predominantly Zn. (6) As is typically observed after exposure to the atmosphere, oxygen was present in all films (typically 2–10 at% relative to Cu), including those prepared from oxygen-free precursors (complexes **4** and **6**).[51] (7) Carbon was present in many of the films (e.g. 0–5% in films deposited using $BEt_3$ or $AlMe_3$). (8) The amount of oxygen and carbon in the films varied greatly depending on the amount of B, Al or Zn incorporated in the film, the susceptibility of each element to oxidation (Al > Zn > B), the nature of the ligands in [$CuL_2$], film thickness, and film morphology (e.g. porosity, grain size and surface coverage).

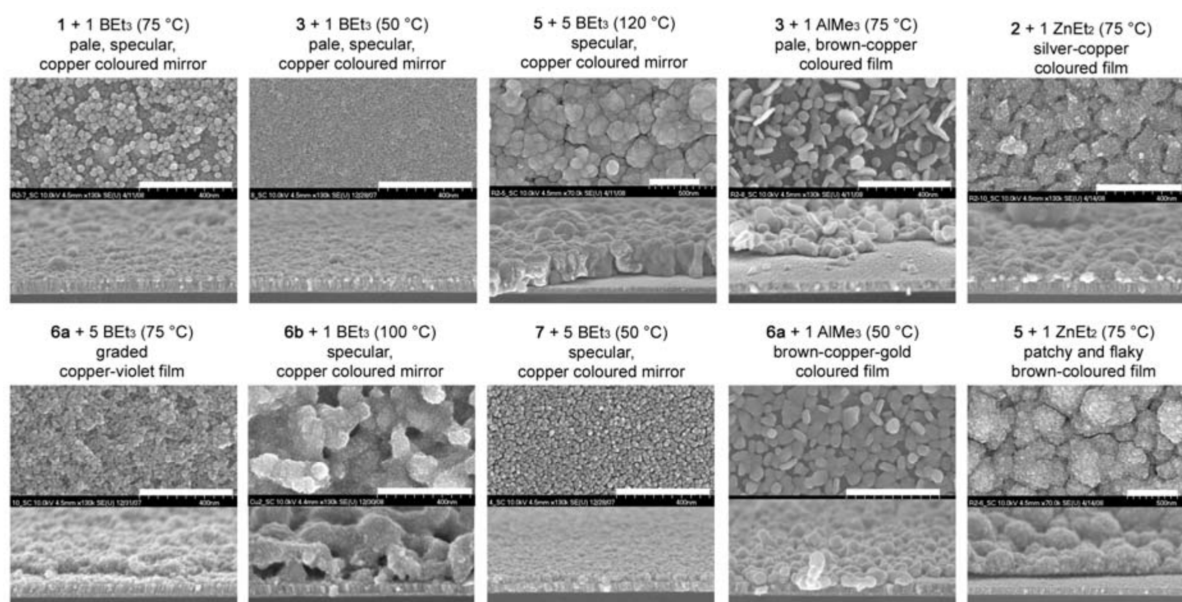


**Figure 5.** SEM images of selected metal films deposited on ruthenium through the reactions of **1**-**7** with $ER_n$ co-reagents in toluene (SEM images for the film deposited through the reaction of **6b** with $ZnEt_2$ in toluene are shown in Figure 6). For each film, the reagents, reaction stoichiometry, reaction temperature, and macroscopic film appearance is provided. White scale bars are set to 400 nm.

These screening studies demonstrate the potential utility of $AlMe_3$, $BEt_3$ and $ZnEt_2$ as new co-reagents for low temperature copper metal ALD or pulsed-CVD, and also the suitability of copper(II) complexes as precursors for copper deposition (see below for ALD/pulsed-CVD studies using $AlMe_3$, $BEt_3$ and $ZnEt_2$ in combination with complex **6b**). Copper(II) precursors are often considered less reactive than copper(I) precursors, but in many cases offer the advantages of straightforward preparation, modification and handling (many are air stable), and higher thermal stability. These studies also highlight the sensitivity of Cu film composition to the nature of the ligands in the [$CuL_2$] precursor and the choice of $ER_n$ co-reagent. However, it is important to note that while in solution, films with lower B, Al or Zn content require the formation of *soluble* and thermally robust B-, Al- and Zn-byproducts, in metal ALD, byproduct *volatility* and thermal stability are key factors in determining the level of B, Al or Zn incorporation. That said, the potential benefits of alloying elements for copper interconnect applications were recently discussed; aluminum is listed in a group of 10 elements of particular interest (Pd, Au, Al, In, Ag, Cr, B, Ti, Nb and Mn), while zinc is included in a list of an additional 6 elements worthy of further investigation (Zn, V, C, Mg, P and Sn).[52]

**Copper Metal ALD/Pulsed-CVD Studies:** Based on solution screening results as well as $CuL_2$ complex properties, the precursor complex bis(*N*-ethyl-2-pyrrolylaldiminate)copper(II) (**6b**) was selected for ALD/pulsed-CVD evaluation with the co-reagents $AlMe_3$, $BEt_3$ and $ZnEt_2$. Desirable features of complex **6b** are volatility, the absence of oxygen or fluorine in the ligands, and good thermal stability; CVD was not observed in the temperature range of interest (≤150 °C).

**Deposition Studies using $AlMe_3$ and $BEt_3$ as Co-Reagents:** At temperatures of 120 – 150 °C using **6b** with $AlMe_3$ as the co-reagent, copper-containing films were deposited via a pulsed-CVD mechanism. However, the resulting films were non-conductive and granular with a high Al and O content (after atmospheric exposure). The lack of electrical conductivity presumably stems from the

presence of insulating $Al_2O_3$ (Al 2*s* binding energy of 119.0 eV). Since the ALD chamber received a two hour forming gas prebake at 250 °C prior to ALD/pulsed-CVD processing, the most likely source of $Al_2O_3$ in the film is the oxidation of metallic Al upon film exposure to air. Similar results were obtained using complex **7** in combination with $AlMe_3$. By contrast, no film was deposited when $BEt_3$ was used as a co-reagent with **6b** or **7**. The observation of deposition with $AlMe_3$, but not $BEt_3$, is in keeping with the order of reactivity observed in solution ($AlMe_3$ >> $BEt_3$). However, factors such as ineffective chemisorption of $BEt_3$ vapors on the surface, or intial surface reactivity that does not result in the formation of active sites suitable to allow further film growth could also play an important role.

**Deposition using $ZnEt_2$ as Co-Reagent:** With $ZnEt_2$ in combination with **6b**, conductive copper films were deposited from 120 °C to 150 °C on $SiO_2$, PVD Ta and PVD Ru substrates. All films are granular with low carbon impurities post sputter (< 2 at%) and no detectable nitrogen, suggesting minimal incorporation of the *N*-ethyl-2-pyrrolylaldiminate or ethyl ligands. In a typical deposition, a pulse sequence consisting of a 6s pulse of $ZnEt_2$ followed by a 7s chamber purge, a 3s pulse of **6b** and a final 7s chamber purge yielded granular films with a growth per cycle of approximately 0.1 Å. As is evident in the SEM images presented in Figure 6, films deposited on $SiO_2$ and PVD Ta substrates at 130 °C are both smooth and uniform. Four point probe sheet resistance measurement of the film on $SiO_2$ combined with a thickness of 120 Å yielded a resistivity of 89 μΩ·cm.

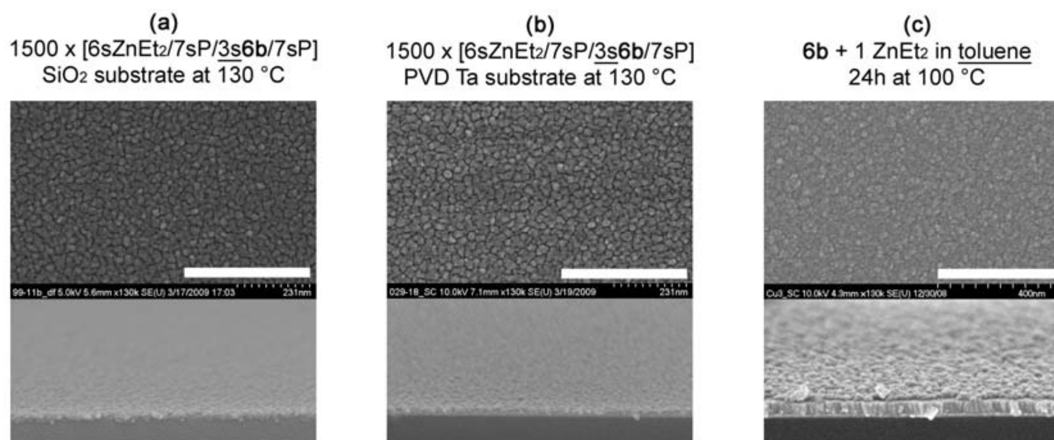

**Figure 6.** (a-b) SEM images of films deposited at 130 °C on $SiO_2$ and PVD Ta, respectively, using 1500 cycles of: 6s pulse $ZnEt_2$ / 7s chamber purge / 3s pulse of **6b** / 7s chamber purge. (c) SEM image of the film deposited on PVD Ru through the reaction of **6b** with 1 equiv. of $ZnEt_2$ in toluene at 100 °C for 24 hours. In figure captions, s = seconds and P = purge. White scale bars are set to 400 nm.

Film composition was analyzed by XPS depth profiling which revealed that Zn was the main film impurity, with no detectable N and less than 2 at% C detected at all sputter depths. Some interesting trends were apparent in the elemental depth profiling (Figure 7). Most prominently, the outer surface of the film was richer in Zn compared to the bulk of the film where a significantly higher concentration of copper was detected. The binding energies for Cu 2*p* and Zn 2*p* on the surface post 30s Ar sputter were 932.6 eV and 1021.9 eV, respectively, which is consistent with the presence of metallic Cu and Zn and/or their oxides $Cu_2O$ and ZnO, respectively.[53] Oxygen was detected at all levels of the depth profile, but the Si/O ratio remains constant after sputtering for 40s, which suggests that in the bulk of the film, copper and zinc are predominantly in metallic form. The observed electrical conductivity of the film also supports the presence of a substantial amount of metallic Cu and/or Zn in the film, most likely alloyed as a brass. As the depth profile shows, the ratio of Cu/Zn in the film was maximized at approximately 11:1. Attempts to further increase the concentration of Cu in the film by varying the substrate temperature between 130 °C and 150 °C, or the length of purges or precursor/co-reactant doses have met with limited success, with Cu:Zn ratios remaining between 6 and 12.

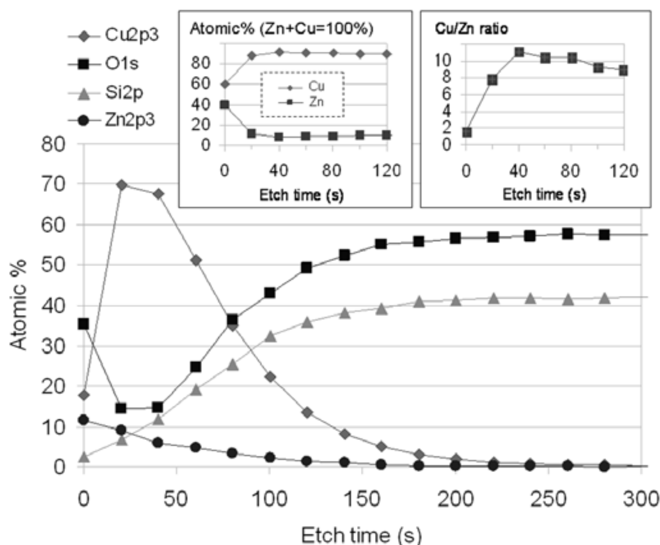


**Figure 7.** XPS determined atomic% compositional depth profile [carbon values were < 2 at% at all sputter depths (20 – 300 s), so are not included in the profile] of film deposited on $SiO_2$ at 130 °C using 1500 cycles of the following pulse sequence: 6s pulse $ZnEt_2$ / 7s chamber purge / 3s pulse of **6b** / 7s chamber purge. The inset on the left plots Zn atomic% and Cu atomic% where the total Zn and Cu content is set to 100%. The inset on the right plots the Cu:Zn ratio against etch time.

The observed Zn content in the film suggests that reductive decomposition of $ZnEt_2$ (or its transmetallation products) is occurring as has been suggested for the $ZnEt_2/H_2O$ ALD ZnO process.[54] Moreover, the increase in Zn concentration close to the surface of the film suggests that this process is self-catalyzed. However, it is also possible that Zn 'percolates' to the surface of the film as it grows, leading to a higher Zn concentration near the surface, even if the Cu/Zn ratio for material added in each deposition cycle remains constant. This type of 'surfactant' behaviour has previously been reported for C in Zn,[55] I in Cu,[56] and $Bi_2O_3$ in $LaAlO_3$.[57]

To gain insight into the process of zinc incorporation into the films, CVD of Zn on a copper substrate was attempted at 100, 120 and 140 °C. At 100 and 120 °C, only a small amount of Zn deposition was observed after 1000 × 1 s pulses, while at 140 °C, CVD of large grains on the surface was observed (Figure 8; zinc deposition was confirmed by XPS). It therefore appears that in

ALD/pulsed-CVD experiments using **6b** in combination with $ZnEt_2$, zinc incorporation occurs via a parasitic CVD pathway[58] that becomes far more pronounced at temperatures of 120 °C and above, detracting from the goal of self-limiting deposition (i.e. leading to a pulsed CVD rather than an ALD process). Along similar lines, while Sung, Koo and Fischer *et al.* reported pure copper metal ALD using $[Cu(OCHMeCH_2NMe_2)_2]$ in combination with $ZnEt_2$ at 100 to 120 °C, substantial zinc incorporation was observed above 120 °C. Unfortunately, with complex **6b**, similarly low deposition temperatures were not accessible due to a minimum precursor delivery temperature of 120 °C.

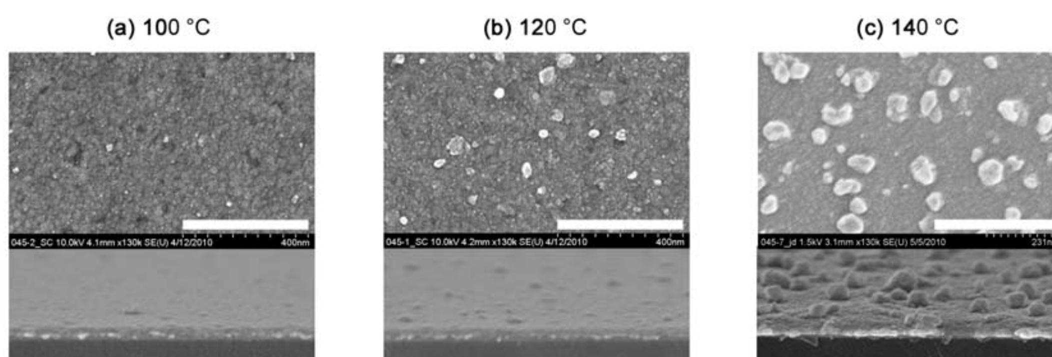


**Figure 8.** SEM images of CVD films deposited on PVD-Cu using $ZnEt_2$ at 100 - 140 °C. Depositions were run using 1000 cycles × [1s pulse $ZnEt_2$ / 3s chamber purge].

**Summary and Conclusions**: A key factor which has hindered the development of new metal ALD/pulsed-CVD methods is the extremely time consuming and resource intensive nature of the process, as well as the requirement for the use of highly specialized equipment. This work demonstrates the usefulness of solution screening methods to identify particularly promising new precursor/co-reagent combinations for metal ALD/pulsed-CVD. Based on the solution data, two precursor/co-reagent combinations were selected for more resource and time intensive ALD/pulsed-CVD studies; $AlMe_3$ and $ZnEt_2$ with bis(*N*-ethyl-2-pyrrolylaldiminate)copper(II) (**6b**). The co-reagent $BEt_3$ was also investigated

to determine whether lower reactivity (relative to $AlMe_3$ and $ZnEt_2$) in solution would translate into reduced ALD/pulsed-CVD reactivity.

As anticipated, no deposition was observed with $BEt_3$. However, with $AlMe_3$, non-conductive (presumably due to the presence of significant $Al_2O_3$ impurities after atmospheric exposure) copper-containing films were deposited between 130 and 150 °C. By contrast, with $ZnEt_2$, deposition of conductive copper metal films was achieved at 130–150 °C. For films deposited on $SiO_2$ at 130 °C using a typical pulse sequence, XPS depth profiling revealed that Zn was the main film impurity, with no detectable N and less than 2 at% C detected at all sputter depths. The maximum copper/zinc ratio was approximately 11:1, with a significant decrease in this ratio near the surface of the film. CVD studies with $ZnEt_2$ point towards the operation of parastic $ZnEt_2$ reduction pathways that become particularly significant at temperatures above 120 °C. Nevertheless, this work highlights the potential of $ZnEt_2$ and related volatile organometallics as co-reagents for low-temperature late transition metal ALD and pulsed-CVD, and demonstrates the successful implementation of solution screening tests to define the focus of ALD/pulsed-CVD studies.

Mechanistic studies to probe in detail the pathways responsible for the solution deposition of copper films using $ZnEt_2$, $AlMe_3$ and $BEt_3$ co-reagents in solution are discussed in a following manuscript.[33] Future studies will focus on strategies to achieve self-limiting deposition and extend these approaches to the ALD/pulsed-CVD of other late transition metals. This work will continue to rely on the high throughput solution screening methodology outlined above, and will target both copper(II) precursors of increased volatility and alternate co-reagents, including new organozinc co-reagents to avoid the reductive decomposition observed with $ZnEt_2$.

**Experimental Section:** An argon-filled MBraun UNIlab glove box was employed for the manipulation and storage of all oxygen and moisture sensitive compounds, and air-sensitive preparative reactions were performed on a double manifold high vacuum line using standard techniques.[59] Residual oxygen

and moisture was removed from the argon stream by passage through an Oxisorb-W scrubber from Matheson Gas Products. A Fisher Scientific Ultrasonic FS-30 bath was used to sonicate reaction mixtures where indicated, and a Fischer Scientific Model 228 Centrific Centrifuge in combination with air-tight Kimble-Kontes 15 mL conical centrifuge tubes was used when required to remove insoluble salts or collect suspended solid for PXRD analysis. Vacuum was measured using a Varian Model 531 Thermocouple Gauge Tube with a Model 801 Controller. Anhydrous 1,2-dme and diethyl ether were purchased from Aldrich. Hexanes, toluene and THF were initially dried and distilled at atmospheric pressure from $CaH_2$, sodium and sodium benzophenone ketyl respectively. Unless otherwise noted, all anhydrous protio solvents were stored over an appropriate drying agent prior to use ($OEt_2$, toluene, $C_6H_6$ = $Na/Ph_2CO$; hexanes = $Na/Ph_2CO$/tetraglyme). $Cu(OMe)_2$, $Cu(OAc)_2$, acetylacetone, 2-pyrrolylaldehyde, salicylaldehyde, isopropylamine, **1** and **2**.$x$$H_2O$ were purchased from either Aldrich or Strem Chemicals. Complexes **1** and **2**.$x$$H_2O$ were obtained from commercial sources, complexes **4-7** were prepared as described in the literature,[16,39,41,42] and complex **3** was prepared from $Cu(OMe)_2$ and H(acnac)[60] by a modification of a procedure reported for a related copper(II) β-ketiminate complex.[61] Purple anhydrous **2** was obtained from green **2**·$x$$H_2O$ by drying under a static vacuum over $P_2O_5$, followed by sublimation.[36,37] $AlMe_3$ (98%), $ZnEt_2$ (min.95%) and $BEt_3$ (98%) were purchased in Sure-Pak cylinders from Strem chemicals and stored within an argon-filled glove box. ***NOTE:*** *$AlMe_3$, $ZnEt_2$ and $BEt_3$ are strongly pyrophoric liquids so must only be handled under strict air-free conditions.*

Combustion elemental analyses were performed on a Thermo EA1112 CHNS/O analyzer, and UV-Visible spectra were performed using a Varian Cary 50 spectrometer. Thermogravimetric analyses were carried out on 3-10 mg of material sealed inside Al crucibles in a nitrogen atmosphere glovebox. Samples were pierced and exposed to the atmosphere for only a few seconds prior to being placed in a stream of high purity Ar in the oven of a standard TGA tool and heated at a rate of 10 °C / min. Room temperature magnetic measurements were performed on a Johnson & Matthey magnetic susceptibility balance, and diamagnetic corrections were applied using Pascal's constants.[62] Single crystal X-ray

crystallographic analyses were performed on crystals coated in Paratone oil and mounted either on: (a) a SMART APEX II diffractometer with a 3 kW Sealed tube Mo generator in the McMaster Analytical X-Ray (MAX) Diffraction Facility, Department of Chemistry, McMaster University, Canada, or (b) a Bruker D8 Platform diffractometer with an APEX CCD detector in the Department of Chemistry and Biochemistry, University of California - San Diego, US. Powder X-Ray Diffraction (PXRD) experiments were performed on a Bruker D8 Advance Powder diffractometer with Cu Kα radiation ($\lambda$ = 0.154 nm) operated at 40 kV and 40 mA.

**[Cu(acnac$^{i\mathrm{Pr}}$)$_2$] (3)** was prepared by a modification of the procedure reported for the *N*-$CH_2CH_2OMe$ analogue:[61] To a solution of H(acnac$^{i\mathrm{Pr}}$) (100 mg, 0.709 mmol) in toluene (10 mL) was added copper(II) methoxide (44.5 mg, 0.355 mmol). The mixture was then stirred overnight to give a red-brown solution. After removal of solvent *in vacuo*, the residue was redissolved in hexanes (5 mL), centrifuged to remove any insoluble impurities, reduced in volume to 2.5 mL, and cooled to –30 °C to yield X-ray quality red-brown crystals of **3** after several days. Yield 95 mg (78%). **Anal. Calcd. for $C_{16}H_{28}N_2O_2Cu$:** C 55.87, H 8.21, N 8.15. Found: C 56.08, H 8.44, N 8.16 %. $\lambda_{max}$ in toluene = 470 nm ($\varepsilon$ = 870 L mol$^{-1}$ cm$^{-1}$). $\mu_{eff}$(solid) = 1.91 BM at 24 °C.

**Solution Deposition Studies:** Solution deposition studies were carried out by addition of either 1.0 or 5.0 equivalents of a 150 mM toluene solution of each co-reagent to 1.0 ml of a 15 mM toluene solution of each copper precursor complex in an 8 ml Kimble-Kontes borosilicate screw-cap culture tube with a phenolic screw cap containing a PTFE-faced rubber liner. The resulting 1:1 reactions were 13.6 mM in copper precursor (1.1 mL total solution volume), while 1:5 reactions were 10 mM in copper precursor (1.5 mL total solution volume). Using a VWR analog dry block heater, reactions were maintained for 24 hours at each of the following temperatures in sequence: 25, 50, 75, 100, 120 °C, and observations were recorded at each of these temperatures. Copper-colored or black powders were analyzed by PXRD and in some cases XPS. Reactions which resulted in the deposition of copper films were repeated in the presence of a Si/$SiO_2$/Ta/Ru wafer section, and the resulting films were analyzed by SEM and XPS.

**Scanning Electron Microscopy (SEM):** All samples were sputter-coated with *ca.* 10 Å of Au/Pd alloy prior to imaging. Imaging was carried out on a standard field-emission electron microscope. Typical working distances were 2.5 – 4.5 mm. For top down images Vacc = 10 kV with 15 μA imaging current. For tilt and X-section images Vacc = 5 kV with 10 μA imaging current.

**X-Ray Photoelectron Spectroscopy (XPS) of films deposited from solution:** X-Ray photoelectron spectra were collected on either a Thermo Scientific Thetaprobe or K-Alpha (Thermo Scientific, E. Grinstead, UK) both of which are located at the University of Toronto. A monochromated Al K-Alpha was used with a spot size of 400 μm. After an initial survey spectrum was collected on the as-is samples, sputter cleaning was performed to remove the surface oxide and any contamination. The cleaning was followed in a profile mode monitoring Cu, O, C and Ru intensities. An Ar ion gun was used with 3 kV energy and rastered over either a 2 mm × 2 mm area (K-Alpha) or a 1.5 mm × 1.5 mm area (Thetaprobe). The profile was continued until the C and O values leveled off, or the underlying Ru layer became apparent. Then the survey spectrum was obtained at low energy resolution for composition (Cu, O, C, Ru, N, Al, B and/or Zn), as well as the high energy resolution spectrum of the Cu $2p_{3/2}$ region (pass energy 10 eV). Because of the different geometries of the spectrometers, the take-off angle (relative to the sample surface) was 90° and 55° for the K-Alpha and Thetaprobe respectively.

**X-Ray Photoelectron Spectroscopy (XPS) of films deposited by ALD/pulsed-CVD:** X-ray photoelectron spectra were collected on a standard XPS tool using a monochromated Al Kα X-ray source and spot size of 400 × 800 μm. Sputtering was performed with a 2 kV Ar+ beam rastered over a 4mm × 4mm area. The sample was grounded at the surface during depth profiling and no charge neutralization was used. Prior to depth profiling, an initial survey spectrum was collected on the as-received sample. Cu 2p, Zn 2p, Si 2p, C 1s, O 1s and N 1s spectra were acquired during the profile. Post sputter, the C 1s signals were located in the baseline indicating less than 2 at% C at all sputter depths and could not be accurately integrated.

**X-Ray Photoelectron Spectroscopy (XPS) of $ZnEt_2$ pulsed CVD films on PVD Ta/Cu substrates:** X-Ray photoelectron spectra were collected on a Thermo Scientific ESCALAB 250 instrument (ThermoScientific, East Grinstead, UK) at the CAMCOR Surface Analytical Facility, University of Oregon. A monochromated Al Kα X-ray source was used with a spot size of 250 μm. Sputtering was performed with a 1kV Ar+ beam rastered over a 2mm x 2mm area. Surfaces were analyzed as received as well as post 15s Ar+ sputter. Cu 2p, Zn 2p, Si 2p, C 1s, O 1s and N1s spectra were acquired. The take-off angle (relative to the sample surface) was 90°.

**Substrates for ALD/pulsed-CVD or CVD Experiments:** Substrates were as follows: i) $SiO_2$: 1 kÅ thermally grown $SiO_2$/Si films were used as received; ii) PVD Ta & PVD Ta/Ru: 1 kÅ thermally grown $SiO_2$/Si substrates received a standard RCA clean prior to the physical sputter of 150 Å Ta or 150 Å Ta plus 370 Å Ru metal without an air-break, respectively; iii) PVD Ta/Cu: 1kÅ $SiO_2$/Si substrates received a standard RCA clean prior to the physical sputter of 100 Å Ta followed by 300 Å Cu without air break. All substrates were exposed to the atmosphere prior to ALD/pulsed-CVD or CVD.

**Atomic Layer Deposition / pulsed-CVD:** ALD/pulsed-CVD experiments were carried out in a standard horizontal, hot wall traveling wave ALD reactor. The chamber received a two hour 250 $^{o}$C nitrogen purge with pulsed forming gas prior to starting ALD/pulsed-CVD deposition. The typical deposition pressure was 30 Pa (0.3 Torr) with 1 slm. $N_2$ (99.999%) carrier gas. Diethylzinc (Crompton GmbH), trimethylaluminum (Crompton GmbH) and triethylborane (Sigma-Aldrich, Inc.) were used as received and were held at room temperature during delivery. The Cu precursor **6b** was held in a solid source vaporizer at 120 $^{o}$C. A schematic of the ALD reactor can be found in the ESI. Typical ALD/pulsed-CVD runs done at 130 $^{o}$C – 150 $^{o}$C substrate temperatures with different co-reactants were as follows: $ZnEt_2$: 1500 × [6s $ZnEt_2$/7s purge/3s **6b**/7s purge]; $AlMe_3$: 1000 × [3s **6b**/7s purge/0.3s $AlMe_3$/7s purge]; $BEt_3$: 5000 × [0.4s $BEt_3$/1.8s purge/1.5s **6b**/1.8s purge]. Samples were cooled to <60 $^{o}$C prior to removal from the reactor.

**CVD using $ZnEt_2$:** CVD studies were carried out on PVD Ta/Cu substrates. Substrates were heated to 150 °C in the same ALD chamber used for the atomic layer deposition/pulsed CVD experiments. Forming gas was flowed through chamber for 500s. The chamber temperature was then stabilized at the desired substrate temperature prior to 1000 cycles of 1s $ZnEt_2$/3s purge.

**Acknowledgements.** DJHE is grateful for funding provided by Intel Corporation and the Emerging Materials Knowledge (EMK) program of Ontario Centres of Excellence (OCE), Canada. We thank Dr. Rana Sodhi of Surface Interface Ontario, University of Toronto, Canada and Dr. Stephen Golledge, CAMCOR, University of Oregon, USA for acquisition of XPS data.

**Supporting Information Available:** Additional surface characterization, experimental details, and X-ray crystallographic data. This material is available free of charge via the internet at http:/pubs.acs.org/.

**References**


(1) Rosenberg, R.; Edelstein, D. C.; Hu, C.-K.; Rodbell, K. P. *Ann. Rev. Mater. Sci.* **2000**, *30*, 229.

(2) Hau-Riege, C. S. *Microelectron. Reliab.* **2004**, *44*, 195.

(3) (a) Kim, H. *Surf. Coat. Technol.* **2006**, *200*, 3104. (b) Carraro, C.; Maboudian, R.; Magagnin, L. *Surf. Sci. Rep.* **2007**, *62*, 499. (c) Shacham-Diamand, Y.; Inberg, A.; Sverdlov, Y.; Bogush, V.; Croitoru, N.; Moscovich, H.; Freeman, A. *Electrochim. Acta* **2003**, *48*, 2987.

(4) *The International Technology Roadmap for Semiconductors*, 2007, Semiconductor Industry Association, http://www.itrs.net/.

(5) Kim, H. *J. Vac. Sci. Technol., B* **2003**, *21*, 2231.

(6) (a) Leskelä, M.; Ritala, M. *Angew. Chem. Int. Ed. Engl.* **2003**, *42*, 5548. (b) Leskelä, M.; Niinistö, L.; Pakkanen, T.; Mason, N. J.; Tischler, M. A.; Bedair, S. M.; Yao, T., In *Atomic Layer Epitaxy*, Suntola, T.; Simpson, M., Eds.; Blackie: Glasgow and London, 1990. (c) Ritala, M.; Leskelä, M., Atomic Layer Deposition. In *Handbook of Thin Film Materials*, Nalwa, H. S., Ed.; Academic Press: San Diego, 2001; Vol. 1 - Deposition and Processing of Thin Films, p 103. (d) Zaera, F. *J. Mater. Chem.* **2008**, *18*, 3521. (e) Kim, H.; Lee, H.-B.-R.; Maeng, W.-J. *Thin Solid Films* **2009**, *517*, 2563. (f) Knez, M.; Nielsch, K.; Niinistö, L. *Adv. Mater.* **2007**, *19*, 3425.

(7) Niinistö, L.; Päiväsaari, J.; Niinistö, J.; Putkonen, M.; Nieminen, M. *Phys. Status Solidi A* **2004**, *201*, 1443.

(8) Hämäläinen, J.; Kemell, M.; Munnik, F.; Kreissig, U.; Ritala, M.; Leskelä, M. *Chem. Mater.* **2008**, *20*, 2903.

(9) Pore, V.; Ritala, M.; Leskelä, M. *Chem. Vapor Depos.* **2007**, *13*, 163 and references therein.

(10) (a) Pore, V.; Hatanpää, T.; Ritala, M.; Leskelä, M. *J. Am. Chem. Soc.* **2009**, *131*, 3478 and references therein. (b) Knapas, K.; Hatanpää, T.; Ritala, M.; Leskelä, M. *Chem. Mater.* **2010**, *22*, 1386.

(11) Thermal ALD of various other classes of material have also been reported, for example arsenides and phosphides (e.g. AlAs, GaAs and InP).

(12) Lee, B. H.; Hwang, J. K.; Nam, J. W.; Lee, S. U.; Kim, J. T.; Koo, S.-M.; Baunemann, A.; Fischer, R. A.; Sung, M. M. *Angew. Chem. Int. Ed. Engl.* **2009**, *48*, 4536.

(13) (a) Li, Z.; Rahtu, A.; Gordon, R. G. *J. Electrochem. Soc.* **2006**, *153*, C787. (b) Li, Z.; Barry, S. T.; Gordon, R. G. *Inorg. Chem.* **2005**, *44*, 1728.

(14) Park, K.-H.; Bradley, A. Z.; Thompson, J. S.; Marshall, W. J. *Inorg. Chem.* **2006**, *45*, 8480.

(15) Park, K.-H.; Marshall, W. J. *J. Am. Chem. Soc.* **2005**, *127*, 9330.

(16) Grushin, V. V.; Marshall, W. J. *Adv. Synth. Catal.* **2004**, *346*, 1457.

(17) Lim, B. S.; Rahtu, A.; Gordon, R. G. *Nat. Mater.* **2003**, *2*, 749.

(18) Lim, B. S.; Rahtu, A.; Park, J.-S.; Gordon, R. G. *Inorg. Chem.* **2003**, *42*, 7951.

(19) Utriainen, M.; Kröger-Laukkanen, M.; Johansson, L.-S.; Niinistö, L. *Appl. Surf. Sci.* **2000**, *157*, 151.

(20) Mårtensson, P.; Carlsson, J.-O. *J. Electrochem. Soc.* **1998**, *145*, 2926.

(21) Mårtensson, P.; Carlsson, J.-O. *Chem. Vap. Deposition* **1997**, *3*, 45.

(22) (a) Goldstein, D. N.; George, S. M. *Appl. Phys. Lett.* **2009**, *95*, 143106. (b) Kim, S.-W.; Kwon, S.-H.; Kwak, D.-K.; Kang, S.-W. *J. Appl. Phys.* **2008**, *103*, 023517. (c) Hämäläinen, J.; Munnik, F.; Ritala, M.; Leskelä, M. *Chem. Mater.* **2008**, *20*, 6840. (d) Ten Eyck, G. A.; Pimanpang, S.; Bakhru, H.; Lu, T.-M.; Wang, G.-C. *Chem. Vap. Deposition* **2006**, *12*, 290. (e) Aaltonen, T.; Ritala, M.; Leskelä, M. *Electrochem. Solid-State Lett.* **2005**, *8*, C99. (f) Aaltonen, T.; Ritala, M.; Sammelselg, V.; Leskelä, M. *J. Electrochem. Soc.* **2004**, *151*, G489. (g) Aaltonen, T.; Ritala, M.; Tung, Y.-L.; Chi, Y.; Arstila, K.; Meinander, K.; Leskelä, M. *J. Mater. Res.* **2004**, *19*, 3353. (h) Aaltonen, T.; Ritala, M.; Sajavaara, T.; Keinonen, J.; Leskelä, M. *Chem. Mater.* **2003**, *15*, 1924. (i) Aaltonen, T.; Ritala, M.; Arstila, K.; Keinonen, J.; Leskelä, M. *Chem. Vap. Deposition* **2004**, *10*, 215. (j) Aaltonen, T.; Alén, P.; Ritala, M.; Leskelä, M. *Chem. Vap. Deposition* **2003**, *9*, 45. (k) Senkevich, J. J.; Tang, F.; Rogers, D.; Drotar, J. T.; Jezewski, C.; Lanford, W. A.; Wang, G.-C.; Lu, T.-M. *Chem. Vap. Deposition* **2003**, *9*, 258. (l) Min, Y.-S.; Bae, E. J.; Jeong, K. S.; Cho, Y. J.; Lee, J.-H.; Choi, W. B.; Park, G.-S. *Adv. Mater.* **2003**, *15*, 1019. (m) Kim, S. H.; Hwang, E. S.; Kim, B. M.; Lee, J. W.; Sun, H. J.; Hong, T. E.; Kim, J. K.; Sohn, H.; Kim, J.; Yoon, T. S. *Electrochem. Solid-State Lett.* **2005**, *8*, C155. (n) Kim, S. H.; Kwak, N.; Kim, J.; Sohn, H. *J. Electrochem. Soc.* **2006**, *153*, G887 and references therein. (o) Klaus, J. W.; Ferro, S. J.; George, S. M. *Thin Solid Films* **2000**, *360*, 145. (p) Grubbs, R. K.; Steinmetz, N. J.; George, S. M. *J. Vac. Sci. Technol., B* **2004**, *22*, 1811.

(23) Wu, L.; Eisenbraun, E. *Electrochem. Solid-State Lett.* **2008**, *11*, H107.

(24) (a) Han, B.; Wu, J.; Zhou, C.; Li, J.; Lei, X.; Norman, J. A. T.; Gaffney, T. R.; Gordon, R.; Roberts, D. A.; Cheng, H. *J. Phys. Chem. C* **2008**, *112*, 9798. (b) Wu, J.; Han, B.; Zhou, C.; Lei, X.; Gaffney, T. R.; Norman, J. A. T.; Li, Z.; Gordon, R.; Cheng, H. *J. Phys. Chem. C* **2007**, *111*, 9403.

(25) An alternative approach which has been used successfully to effect ALD of various metals (e.g. Ta, Ti, Al, Co and Cu) at lower temperatures is the use of plasma to generate radicals (e.g. atomic hydrogen) from co-reagents such as $H_2$ and $NH_3$. This technique is referred to as radical-enhanced ALD (REALD) or plasma-enhanced ALD (PEALD): reference 5.

(26) Li, Z.; Gordon, R. G. *Chem. Vap. Deposition* **2006**, *12*, 435.

(27) (a) Soininen, P. J.; Elers, K.-E.; Haukka, S. U.S. Patent 6,482,740 B2, 2002. Kostamo, J.; Stokhof, M. U.S. Patent 7,067,407 B2, 2006. (b) Huo, J.; Solanki, R.; McAndrew, J. *J. Mater. Res.* **2002**, *17*, 2394. (c) Solanki, R.; Pathangey, B. *Electrochem. Solid-State Lett.* **2000**, *3*, 479.

(28) Bradley, A. Z.; Thompson, J. S. World Patent WO 094689 A2, 2004.

(29) Bradley, A. Z.; Thorn, D. L.; Thompson, J. S. World Patent WO 095701 A1, 2003.
(30) Other reagents including BBN, $B_2H_6$, $BR_xH_{(3-x)}$, dihydrobenzofuran, pyrazoline, disilane, $SiH_4$, $SiR_xH_{(4-x)}$ and $GeR_xH_{(4-x)}$ are also mentioned in references 28 and 29.
(31) Thompson, J. S.; Zhang, L.; Wyre, J. P.; Brill, D. J.; Lloyd, K. G. *Thin Solid Films* **2009**, *517*, 2845.
(32) Kang, S.-W.; Yun, J.-Y.; Chang, Y. H. *Chem. Mater.* **2010**, *22*, 1607.
(33) Vidjayacoumar, B.; Emslie, D. J. H.; Blackwell, J. M.; Clendenning, S. B.; Britten, J. F. - companion article submitted to *Chem. Mater.* in **2010**.
(34) $AlMe_3$ (b.p. 125 °C) was selected, rather than $AlEt_3$ (b.p. 186 °C), due to the greatly reduced cost of pure material and a lower boiling point. Liquid $BEt_3$ (b.p. 95 °C) was used, rather than gaseous $BMe_3$ (b.p. –20 °C), for more straightforward handling. $ZnEt_2$ (b.p. 117 °C) was also selected, rather than $ZnMe_2$ (b.p. 45 °C), for more straightforward handling.
(35) Lebrun, P. C.; Lyon, W. D.; Kuska, H. A. *J. Crystallogr. Spectrosc. Res.* **1986**, *16*, 889.
(36) (a) Bertrand, J. A.; Kaplan, R. I. *Inorg. Chem.* **1966**, *5*, 489. (b) Funck, L. L.; Ortolano, T. R. *Inorg. Chem.* **1968**, *7*, 567.
(37) Maverick, A. W.; Fronczek, F. R.; Maverick, E. F.; Billodeaux, D. R.; Cygan, Z. T.; Isovitsch, R. A. *Inorg. Chem.* **2002**, *41*, 6488.
(38) McGeachin, S. G. *Can. J. Chem.* **1968**, *46*, 1903.
(39) Perry, C. L.; Weber, J. H. *J. Inorg. Nucl. Chem.* **1971**, *33*, 1031.
(40) (a) Holm, R. H.; Chakravorty, A.; Theriot, L. J. *Inorg. Chem.* **1966**, *5*, 625. (b) Yokoi, H.; Addison, A. W. *Inorg. Chem.* **1977**, *16*, 1341.
(41) Sacconi, L.; Ciampolini, M. *J. Chem. Soc.* **1964**, 267.
(42) Orioli, P. L.; Sacconi, L. *J. Am. Chem. Soc.* **1966**, *88*, 277.
(43) Pinkas, J.; Huffman, J. C.; Bollinger, J. C.; Streib, W. E.; Baxter, D. V.; Chisholm, M. H.; Caulton, K. G. *Inorg. Chem.* **1997**, *36*, 2930.
(44) (a) Wei, C. H. *Inorg. Chem.* **1972**, *11*, 2315. (b) Wansapura, C. M.; Choi, J. Y.; Simpson, J. L.; Szymanski, D.; Eaton, G. R.; Eaton, S. S.; Fox, S. *J. Coord. Chem.* **2003**, *56*, 975.
(45) Complex **3** is red-brown with a λmax of 470 nm ($\varepsilon$ = 870 L $mol^{-1}$ $cm^{-1}$), which is an unusually low wavelength absorption for a copper(II) complex, and is also unexpected given literature reports for related $[Cu(acnac)_2]$ compounds: the *N*-methyl analogue is reported to be a grey powder or dark green crystals, the *N*-$CH_2OMe$ analogue is dark green-black, the *N*-Ph analogue is black and the *N*-2,6-diisopropylphenyl derivative is dark green. Given the paramagnetic nature of **3** ($\mu_{eff}$ 1.91 B.M. at 24 °C), the solid state structure was determined in order to verify the identity of the complex. (a) Holtzclaw, H. F., Jr.; Collman, J. P.; Alire, R. M. *J. Am. Chem. Soc.* **1958**, *80*, 1100. (b) Baidina, I. A.; Stabnikov, P. A.; Vasiliev, A. D.; Gromilov, S. A.; Igumenov, I. K. *J. Struct. Chem.* **2004**, *45*, 671. (c) Baxter, D. V.; Caulton, K. G.; Chiang, W.-C.; Chisholm, M. H.; DiStasi, V. F.; Dutremez, S. G.; Folting, K. *Polyhedron* **2001**, *20*, 2589. (d) Hsu, S. H.; Li, C. Y.; Chiu, Y. W.; Chiu, M. C.; Lien, Y. L.; Kuo, P. C.; Lee, H. M.; Huang, J. H.; Cheng, C. P. *J. Organomet. Chem.* **2007**, *692*, 5421.
(46) The elucidation of ALD mechanisms faces many challenges due to the metrology restrictions placed on chemical analysis inside an ALD reactor as well as the very small quantities of surface species and vapor-phase byproducts. The ability to monitor solution-based reactivity between a metal precursor and coreagent by standard techniques including NMR spectroscopy and X-ray crystallography may offer a powerful approach to gain insight into the mechanisms behind atomic layer deposition processes, especially those occurring at low temperatures (e.g. $<150$ °C).
(47) Successful metal deposition is only reported in Figure 4 when a significant quantity of copper was deposited by visual inspection. Given that each reaction involved only 4-6 mg (15 μmol) of the copper precursor, this corresponds to deposition of a substantial percentage of the copper metal present.

(48) Both $AlMe_3$ and $ZnEt_2$ reacted with **6a** within seconds at –78 °C. However, the rate of copper deposition was determined by the thermal stability of the copper(I) alkyl complex, $[CuR]_n$ that formed *en route* to copper metal: reference 33.

(49) Shimizu, S.; Murakami, Y.; Kachi, S. *J. Phys. Soc. Jpn.* **1976**, *41*, 79.

(50) Colloidal brass (5-65 at% Zn in Cu) has been prepared either by addition of an octylamine solution of $[Cu(OCHMeCH_2NMe_2)_2]$ and $ZnEt_2$ to hexadecylamine at 250 °C, or by sequential addition of octylamine solutions of $[Cu(OCHMeCH_2NMe_2)_2]$ and then $ZnEt_2$ to hexadecylamine at 250 °C. Pure colloidal copper and zinc were also accessible by addition of an octylamine solution of just $[Cu(OCHMeCH_2NMe_2)_2]$ or $ZnEt_2$ to hexadecylamine at 250 °C: Hambrock, J.; Schröter, M. K.; Birkner, A.; Wöll, C.; Fischer, R. A. *Chem. Mat.* **2003**, *15*, 4217.

(51) Repeating XPS measurements on several freshly prepared films (from $BEt_3$ with **1**, **6** and **7**) that had been exposed to air for 5-10 minutes, rather than 2 weeks, did not show significantly lower levels of oxygen or carbon.

(52) Barmak, K.; Cabral, C., Jr.; Rodbell, K. P.; Harper, J. M. E. *J. Vac. Sci. Technol., B* **2006**, *24*, 2485.

(53) Hoque, E.; DeRose, J. A.; Houriet, R.; Hoffmann, P.; Mathieu, H. J. *Chem. Mater.* **2007**, *19*, 798.

(54) Rowlette, P. C.; Allen, C. G.; Bromley, O. B.; Dubetz, A. E.; Wolden, C. A. *Chem. Vap. Deposition* **2009**, *15*, 15, and references therein.

(55) Cheon, J.; Dubois, L. H.; Girolami, G. S. *Chem. Mater.* **1994**, *6*, 2279.

(56) Chang, T.-Y.; Tze, J.-J.; Tsai, D.-S. *Appl. Surf. Sci.* **2004**, *236*, 165.

(57) Molodyk, A. A.; Korsakov, I. E.; Novojilov, M. A.; Graboy, I. E.; Kaul, A. R.; Wahl, G. *Chem. Vap. Deposition* **2000**, *6*, 133.

(58) Juppo, M.; Ritala, M.; Leskelä, M. *J. Vac. Sci. Technol. A* **1997**, *15*, 2330.

(59) Burger, B. J.; Bercaw, J. E., Vacuum Line Techniques for Handling Air-Sensitive Organometallic Compounds. In *Experimental Organometallic Chemistry - A Practicum in Synthesis and Characterization*, American Chemical Society: Washington D.C., 1987; Vol. 357, p 79.

(60) Tian, X.; Goddard, R.; Pörschke, K.-R. *Organometallics* **2006**, *25*, 5854.

(61) Baxter, D. V.; Caulton, K. G.; Chiang, W.-C.; Chisholm, M. H.; DiStasi, V. F.; Dutremez, S. G.; Folting, K. *Polyhedron* **2001**, *20*, 2589.

(62) (a) O'Connor, C. J. *Prog. Inorg. Chem.* **1982**, *29*, 203. (b) Pascal, P. *Ann. Chim. Phys.* **1910**, *19*, 5.

**For Table of Contents Use Only (max 75 words; 4x1 inch rectangle for graphics)**

**Investigation of $AlMe_3$, $BEt_3$ and $ZnEt_2$ as Co-Reagents for Low-Temperature Copper Metal ALD / Pulsed-CVD**

**TOC Text:** The reactions of $AlMe_3$, $BEt_3$ and $ZnEt_2$ with toluene solutions of eight copper(II) complexes were investigated, and most combinations were found to deposit metal films or metal powder at 50 $^{o}$C or less. SEM and XPS of metal films deposited on ruthenium showed a range of morphologies and compositions, including pure copper (excluding oxygen content after atmospheric exposure). These non-aqueous solution screening studies provided a rapid and convenient means to identify the most promising [$Cu^{II}L_2$] precursor / $ER_n$ co-reagent combinations for copper metal ALD/pulsed-CVD. Subsequent ALD/pulsed-CVD studies were performed using **6b** in combination with $AlMe_3$, $BEt_3$ and $ZnEt_2$. Of these three co-reagents, $ZnEt_2$ proved the most effective, depositing smooth, conductive copper films (containing 8–15% Zn relative to Cu) at 130 to 150 °C. Based on CVD studies with $ZnEt_2$ on PVD-copper, zinc content appears to derive from a parasitic CVD process which becomes more favorable at temperatures above 120 °C.

**TOC Graphic**